ELSEVIER

Nanosized and delayered zeolitic materials for the liquid-phase Beckmann rearrangement of cyclododecanone oxime

P. Botella [a], A. Corma [a,*], S. Iborra [a], R. Montón [a], I. Rodríguez [b], V. Costa [c]

[a] *Instituto de Tecnología Química, UPV-CSIC, Universidad Politécnica de Valencia, Avda. de los Naranjos s/n, E-46022 Valencia, Spain*
[b] *Centro Tecnológico de Ondas, Unidad Asociada CSIC-UPV, Universidad Politécnica de Valencia, Avda. de los Naranjos s/n, E-46022 Valencia, Spain*
[c] *UBE Corporation Europe, S.A., P.O. Box 118, E-12080 Castellon, Spain*

Abstract

The Beckmann rearrangement of the relatively bulky cyclododecanone oxime was carried out in batch and fixed-bed continuous reactors. With microporous molecular sieve catalysts, the process is controlled by diffusion within the micropores. Conversion, selectivity, and catalyst life are improved with the use of nanocrystalline materials. A solid acid catalyst formed by nanolayers of zeolite is more active and selective than either a nanocrystalline Beta zeolite or a mesoporous MCM-41 material, and the amount of organic remaining adsorbed on the catalyst after reaction is smaller in the former. Product desorption, activity, selectivity and catalyst life are much improved by using a nonprotic polar solvent and higher reaction temperatures.

© 2007 Elsevier Inc. All rights reserved.

Keywords: Beckmann rearrangement; Cyclododecanone oxime; Zeolite nanocrystals; Layered materials; ITQ-2

1. Introduction

The rearrangement of aliphatic ketoximes to lactams in highly concentrated sulphuric acid, known as the Beckmann rearrangement, is a process used industrially for the preparation of lactams, particularly for the preparation of ε-caprolactam and ω-laurolactam. In such a process, the lactam is recovered from the reaction mixture by neutralizing the oleum with aqueous ammonia and then extracting the lactam from the ammonium sulphate solution. A disadvantage of this process is the production of a large quantity of ammonium sulphate; for instance, in the production of ε-caprolactam, 1.7–1.9 ton of $(NH_4)_2SO_4$ per ton of lactam is obtained as a byproduct [1], making commercialisation of this product difficult in some cases. Moreover, the use of large amounts of fuming sulphuric acid and the corresponding problems of corrosion make this process less environmentally friendly than desired.

To overcome these drawbacks, attempts have been at replacing sulphuric acid by solid acid catalysts—specifically, zeolites—because these materials can be synthesized with various crystalline structures, pore dimensions, and different levels of acidities. Among them, Faujasite [2,3], Beta [4,5], Pentasil [8–15], and Mordenite zeolites [11] and the mesoporous molecular sieves MCM-41 [16] and SBA-15 [17] have been tested with different success for the liquid and vapor-phase Beckmann rearrangement of cyclohexanone oxime. When working in vapor phase, the reaction must be carried out at high temperatures (523–623 K) to keep the oxime and products in vapor phase. Under these conditions, a high-silica MFI zeolite has given good results and is the basis for Sumitomo Chemicals' first vapor-phase commercial process started in 2000. MFI with pore diameter of 0.53×0.56 nm has shown interesting properties for the Beckmann rearrangement of cyclohexanone oxime to ε-caprolactam, but has strong diffusion limitations when oximes with larger molecular sizes are involved. This is even more significant if one takes into account that in the case of another industrially important lactam, such as ω-laurolactam, the reaction cannot be carried out in the gas phase due to the instability

---

of the precursor oxime, unless the reaction is carried out in vacuum [18]. Recent studies have shown that cyclododecanone oxime can be transformed into ω-laurolactam by using solid catalysts such as rare earth triflate catalysts [19], heteropolyacid catalysts [20], acid-treated mesoporous silicoaluminate catalysts [21], and Beta zeolite [18]. In the case of Beta zeolite, the reaction was carried out at a vacuum of 50 mbar, and temperatures were always above 573 K to decrease the rate of deactivation. Nevertheless, the activity of Beta zeolite for laurolactam production decreased with reaction time.

Attempts to improve the diffusion of reactants to the catalytic sites of zeolites have so far been focused on increasing pore size [22], creating mesoporosity, and decreasing zeolite crystal size. Recent work has described new zeolitic materials [23,24] in which a layered zeolite precursor [6,25,26] is delayered. This process results in well-defined aluminosilicate nanolayers with very large external surface areas ($>500\ \text{m}^2\ \text{g}^{-1}$) with catalytic sites accessible to large molecules while allowing rapid desorption of products.

In the present work, we studied the liquid-phase Beckmann rearrangement of cyclododecanone oxime (CDOX) into 2-azacyclotridecanone or ω-laurolactam (LRL), which is the monomer of Nylon-12. We studied the process in both a batch reactor and a fixed-bed, continuous-flow reactor. To explore the possibilities of different types of catalysts in which active site accessibility can play an important role, instead of the medium-pore MFI, we used a large-pore Beta and a nanocrystalline Beta zeolite as catalysts. We then studied the catalytic behaviour of materials with a larger "external" surface area, such as mesoporous molecular sieves and a delaminated nanolayered zeolitic material with a highly structured external surface area. Finally, we explored the combined affect of accessibility and solvent polarity on catalyst life.

2. Experimental

2.1. Materials

ITQ-2, Si/Al = 15, 25, and 50 (M) and MCM-22, Si/Al = 15 (M), were prepared from the corresponding laminar precursors with the MWW structure [6,7,23]. The MCM-41 sample with an Si/Al ratio of 50 (M) and a pore diameter of 3.5 nm was prepared as described previously [27].

Beta zeolite, Si/Al = 50 (M) (Beta-50), was synthesized hydrothermally at 413 K, using tetraethylammonium (TEA$^+$) as a structure-directing agent and F$^-$ as silica mobilizing agent [28]. A nanocrystalline Beta sample with Si/Al = 16 (M) and crystal size of 20 nm (Beta-n) was synthesized as described previously [29]. Finally, a commercial sample of Beta zeolite (Beta-CP811) was provided by PQ-Zeolyst.

Crystallinity and phase purity of solids were determined by powder X-ray diffraction (XRD) patterns using a Philips X'Pert diffractometer equipped with a graphite monochromator, operating at 40 kV and 45 mA and using nickel-filtered Cu$K\alpha$ radiation ($\lambda = 0.1542$ nm). Liquid nitrogen adsorption isotherms of the 200-mg samples were measured in a Micromeritics Flowsorb apparatus. Samples for transmission electron microscopy

Table 1
Crystalline and textural characteristics of catalysts

Catalysts	Si/Al	Crystal size[a] (nm)	V_{total} (cm^3 g^{-1})	ESA[b] (m^2 g^{-1})
Beta-CP811	12.5	150	0.59	209
Beta-50	50	500	0.19	96
Beta-n	16	20	0.20	168
MCM41	50	<100	0.58	60
ITQ-2(50)	50	300	0.87	618
ITQ-2(25)	25	400	0.68	373
ITQ-2(15)	15	500	0.77	348
MCM-22(15)	15	500	0.59	141

[a] Derived from SEM images.
[b] External surface area.

Table 2
Brønsted (B) and Lewis (L) acidity of catalysts measured by IR spectroscopy combined with pyridine adsorption and desorption at different temperatures

Catalyst	Si/Al	Acidity[a]					
		423 K		523 K		623 K	
		B	L	B	L	B	L
Beta-CP811	12.5	nd[b]	nd[b]	45	48	27	40
Beta-50	50	10	21	8	18	4	5
Beta-n	16	35	58	33	46	30	26
MCM-41	50	11	6	8	2	2	0
ITQ-2(50)	50	21	19	12	11	14	6
ITQ-2(25)	25	22	50	19	41	17	31
ITQ-2(15)	15	28	67	27	67	21	39
MCM-22(15)	15	58	38	51	28	38	27

[a] $\mu\text{mol}_{\text{py}}\ \text{g}_{\text{cat}}^{-1}$. Calculated using the extinction coefficients given in Ref. [43].
[b] Not determined.

(TEM) were ultrasonically dispersed in 2-propanol and transferred to carbon-coated copper grids. TEM micrographs were collected in a Philips CM-10 microscope operating at 100 kV. Crystal size was determined from scanning electron microscopy (SEM) images using a JEOL 6300 microscope. Infrared spectra were recorded at room temperature in a Nicolet 710 FTIR using self-supported wafers of 10 mg cm^{-2}. The calcined samples were evacuated overnight at 673 K and 10^{-3} Pa dynamic vacuum; pyridine was then admitted into the cell at room temperature. After saturation, the samples were evacuated at 423, 523, and 623 K for 1 h under vacuum and cooled to room temperature, and the spectra were recorded.

The most relevant physicochemical characteristics of catalysts used in this work are summarized in Tables 1 and 2.

2.2. Reagents

Cyclododecanone oxime was prepared by reaction of the corresponding ketone with hydroxylamine hydrochloride in a mixture of ethanol and pyridine at 358 K according to the general method reported in the literature [30]. The oxime was recrystallized in ethanol before use. The purity (99%) was confirmed by gas chromatography (GC) (Varian 3900 GC, HP-5 column) and mass spectrometry (GC–MS) (Varian Star 3400 GC, HP-5 column). All other reagents were supplied by Aldrich.

2.3. Reaction procedure and product characterization

Batch testing was carried out in a 25-ml glass three-necked flask. A solution of oxime (100 mg) and decane (50 mg, internal standard) in 20 ml of the corresponding solvent (chlorobenzene, 1,3,5-triisopropylbenzene, or benzonitrile) was heated at 403 K. Then the catalyst (100–200 mg), which had been previously activated by heating the solid at 573 K under vacuum (10^3 Pa) for 2 h, was introduced. The resulting suspension was stirred magnetically and refluxed at the reaction temperature. Samples were taken at intervals. At the end of the reaction, the catalyst was filtered and washed with dichloromethane. The organic solution was concentrated in vacuum, and the residue was weighed.

Fixed-bed experiments were carried out at atmospheric pressure in a tubular stainless steel reactor (300 mm long, 10.5 mm i.d.). Typically, 1.00–2.50 g of powder catalyst was pelletized, crushed, and sieved to a particle size of 0.42–0.59 mm. A solution of cyclododecanone oxime in 1,2,4-trimethylbenzene or benzonitrile (3–5 wt%) was fed with a syringe pump. Products and nonreacted oxime flowed down and were recovered and weighed at intervals in a cooling system.

Reaction samples were analyzed by GC in a Varian 3900 gas chromatograph equipped with a HP-5 column and a flame ionization detector. Products were identified by GC–MS using a Varian Saturn II with a Varian Star 3400 gas chromatograph equipped with a HP-5 column and using reference samples.

After reaction, the catalysts exhibited a brownish aspect due to adsorbed products. Reversibly adsorbed products can be recovered by continuous solid–liquid extraction with chloroform for 16 h in a micro-Soxhlet system. After the solvent was removed, the residue was weighted and analyzed by GC–MS. The extract revealed mainly LRL and cyclododecanone (CD), along with traces of cyclododecen-1-one and cyclododecen-1-ol. However, the amount of products collected in the extraction was rather small (about 3–4 wt% of the total CDOX fed).

Elemental analysis was used for carbon determination. The organic deposit was also characterized by ^{13}C CP-MAS-NMR spectroscopy. Spectra were recorded at room temperature under magic-angle spinning on a Bruker AV400 spectrometer. The ^{1}H to ^{13}C cross-polarization spectra were acquired using a 90° pulse for ^{1}H of 5 ms, a contact time of 5 μs, and a recycle time of 3 s. All spectra were recorded with a 7-mm Bruker BL-7 probe at a sample spinning rate of 5 kHz. Spectra were referred to adamantine.

Accordingly, to perform the mass balance of CDOX, the C-content determined by elemental analysis was considered in terms of LRL content, with the corresponding molar quantity added to that obtained in the liquid phase.

Taking into account all of the foregoing considerations, CDOX conversion, selectivity to LRL and hydrolysis products (mainly CD), and CDOX mass balance were calculated according to the following expressions:

– CDOX conversion (%):

$$X_{TCDOX} = \frac{molCDOX_o - molCDOX_f}{molCDOX_o} \times 100,$$
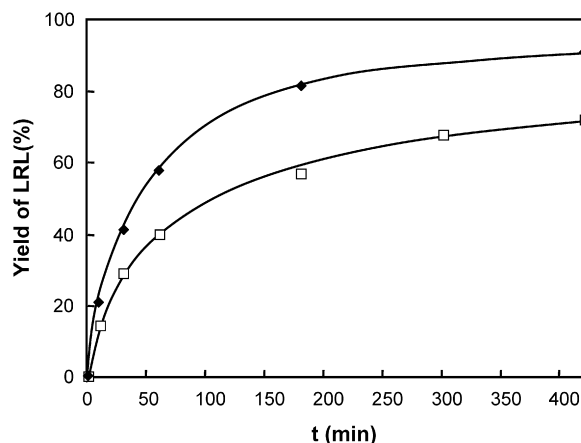

Fig. 1. Beckmann rearrangement of CDOX at 403 K in chlorobenzene and a catalyst/oxime ratio of 1:1 (wt/wt) over ITQ-2(15) (◆) and MCM-22(15) (□).

where $CDOX_o$ is the amount of cyclododecanone oxime fed and $CDOX_f$ the amount detected in the reaction samples.

– LRL selectivity (%):

$$S_{LRL} = \frac{molLRL}{\sum mol(LRL + CD)} \times 100.$$

– CD selectivity (%):

$$S_{CD} = \frac{molCD}{\sum mol(LRL + CD)} \times 100.$$

– CDOX total mass balance (liquid phase and catalyst) (%):

$$MB_{CDOX}$$
$$= \frac{\sum mol(CDOX_f + LRL + molCD) + molLRL_{EA}}{molCDOX_o}$$
$$\times 100,$$

where LRL_{EA} is the molar quantity of ω-laurolactam corresponding to the C-content detected by elemental analysis.

3. Results and discussion

3.1. Beckmann rearrangement of CDOX in a batch reactor

It has been reported [23] that the structure of ITQ-2 zeolite consists of thin sheets (∼2.5 nm thick) with a hexagonal array of "cups" that penetrate into the sheet from both sides. These cups have an aperture of ∼0.7 nm, formed by a 12-membered ring with ∼0.7 nm deep. The cups meet at the centre of the layer, forming a double 6-ring window that connects the cups bottom to bottom, resulting in 10-membered ring channel system that runs in between the cups inside the sheet. Clearly, the benefit of this structure is the greater accessibility and smaller diffusion path to active sites located at the cups. This is demonstrated by comparing the catalytic activities of ITQ-2 and its MCM-22 counterpart (Fig. 1). During the reaction, the only product observed in the liquid phase was the corresponding amide, LRL (Scheme 1). Moreover, Fig. 2 plots the yields of LRL versus time for the Beckmann rearrangement with ITQ-2,

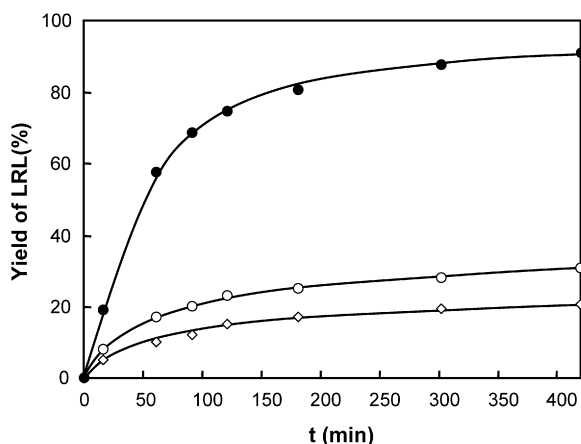**(1) Beckmann Rearrangement**
(2) Hydrolysis
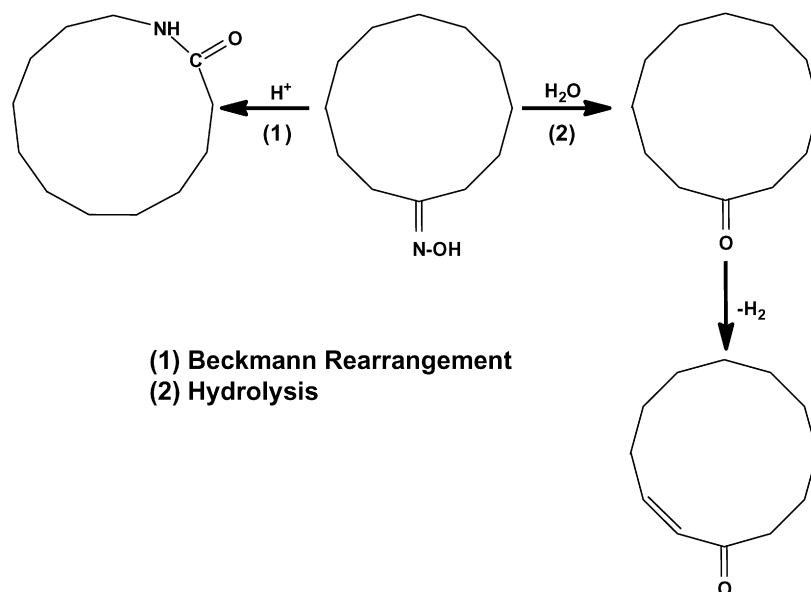
Scheme 1.

Fig. 2. Beckmann rearrangement of CDOX at 403 K in chlorobenzene and a catalyst/oxime ratio of 1:1 (wt/wt) over ITQ-2(50) (●), MCM-41 (○) and Beta-50 (◇).

MCM-41, and Beta zeolite (Beta-50), all of which have a Si/Al molar ratio of 50. As can be seen, ITQ-2 is able to successfully perform the Beckmann rearrangement, achieving a 90% lactam yield after 7 h of reaction time with a selectivity of 100%. The other two catalysts also gave 100% selectivity to the lactam, but their activity was much lower. The lower activity of Beta zeolite should be attributed to the existence of pore geometric constraints for the diffusion of CDOX (molecular size, $1.08 \times 0.95 \times 0.85$ nm) and the corresponding lactam (LRL) (molecular size, $1.04 \times 0.94 \times 0.86$ nm). In this case, adsorbed products can block the pores, leading to rapid deactivation of the catalyst (see Fig. 2).

In the case of MCM-41 catalyst, we cannot expect any diffusion control of reactant or products, because this material has a pore diameter of 3.5 nm. Therefore, its lower activity with respect to ITQ-2 should be attributed to differences in the nature and strength of acid sites on ITQ-2 and MCM-41 catalysts,

as well as to differences in the catalyst deactivation rate, as we discuss later.

Numerous publications on the vapor-phase Beckmann rearrangement of cyclohexanone oxime using solid acid catalysts focus on the nature and strength of the sites responsible for this reaction [31]. Earlier papers suggested that amide formation is catalysed by sites of medium to strong acidity [3,32]. However, later studies [4,11] showed that catalytic activity and selectivity to lactam increase with increasing Si/Al ratio in H-ZSM-5 zeolite. More recently, it has been proposed that the rearrangement of cyclohexanone oxime can be catalysed by even very weak acid sites, such as the internal silanols of zeolites [5,9]. However, performing the Beckmann rearrangement in the liquid phase at moderate temperatures requires greater acid strength compared with that needed to perform the reaction at higher temperatures in the vapor phase [33]. Indeed, in recent work in which the Beckmann rearrangement of cyclohexanone oxime was carried out in solution at moderate temperature in presence of Beta zeolites, it was found that weakly acidic and/or internal silanol groups can catalyse the Beckmann rearrangement, but that bridging hydroxyl groups were more active [5].

Taking these findings into account, we can explain the different activity exhibited by ITQ-2 and MCM-41 considering that MCM-41 sample, due to its short-range amorphous characteristics and easier dealumination during calcination, should have fewer sites with weaker acidity than ITQ-2 zeolite. We checked this by pyridine adsorption–desorption; the results, presented in Table 2, show that indeed the acidity of MCM-41 is not only smaller in number, but also weaker in strength than that of Beta or ITQ-2 zeolites.

3.1.1. Influence of Si/Al molar ratio of ITQ-2 material

A very important parameter that controls the activity and selectivity of zeolites is the Si/Al ratio. This parameter not only defines the number of potential protons, and thus the number and strength of acid sites, but also determines the adsorption
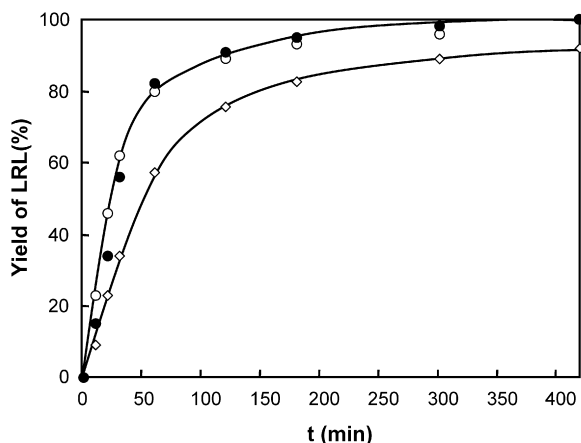
Fig. 3. Beckmann rearrangement of CDOX at 403 K in chlorobenzene and a catalyst/oxime ratio of 1:1 (wt/wt) over ITQ-2(50) (◇), ITQ-2(25) (●) and ITQ-2(15) (○).
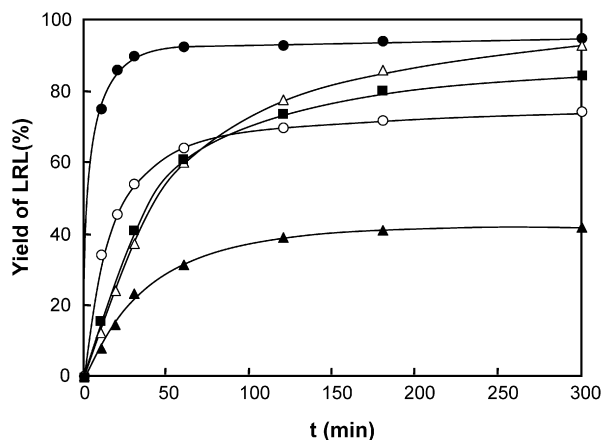

Fig. 4. Beckmann rearrangement of CDOX at 403 K in chlorobenzene and a catalyst/oxime ratio of 2:1 (wt/wt) over ITQ-2(50) (●), MCM-41(50) (○), Beta-CP811 (■), Beta-n (△) and Beta-50 (▲).
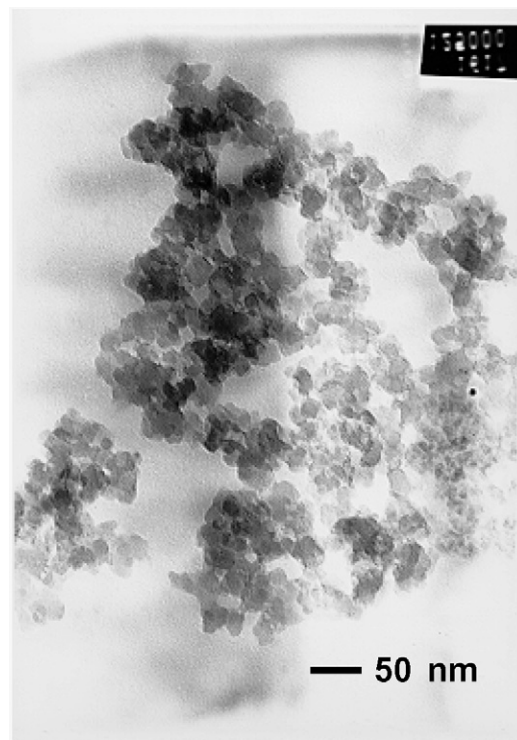

Fig. 5. TEM micrograph of the nanocrystalline Beta-n material.
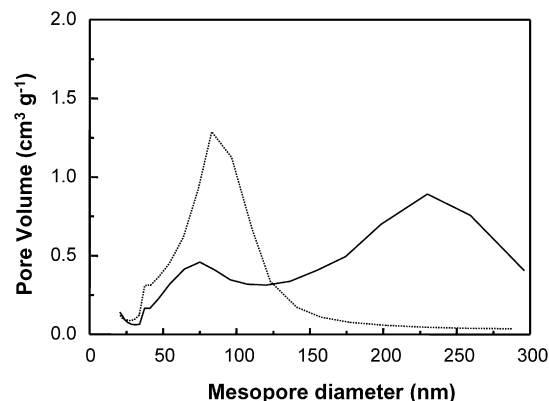
Fig. 6. Pore size distribution of catalysts Beta-50 (—) and nanocrystalline Beta-n (···).

properties of the zeolite. One important advantage of using acid zeolites as catalysts is that they can be prepared in a wide range of Si/Al ratios, making it possible to optimize the catalyst from the standpoint of acid strength and hydrophobic–hydrophilic character for a given reaction. To study the influence of this parameter, we carried out the reaction using delaminated material, ITQ-2, with different Si/Al ratios.

Fig. 3 summarizes the results obtained for the Beckmann rearrangement of CDOX using ITQ-2 samples with Si/Al molar ratios of 15, 25, and 50. As can be seen, the order of activity is ITQ-2(25) ⩾ ITQ-2(15) > ITQ-2(50), which demonstrates a compromise between the level of dealumination (and hence external surface area and molecular accessibility) and acidity (see Tables 1 and 2).

In the case of zeolites, active site accessibility for larger molecules can be improved by increasing the ratio of external surface to internal surface. One way to achieve this is by synthesizing samples with smaller crystallite sizes. Accordingly, we prepared a nanocrystalline Beta zeolite with crystallite size of 20 nm (Beta-n) and tested it for reactivity (Fig. 4). The crystallite agglomeration was less in the nanosample than in a regular

Beta catalyst (Beta-50) (see Fig. 5 and Ref. [29]). Fig. 6 shows that these nanocrystallites generate a system of mesopores with a relatively narrow pore size distribution. This system of pores with significant external surface area ($168 \text{ m}^2 \text{ g}^{-1}$) should allow the reactants to diffuse and reach a relatively larger number of pore mouth channels than in the case of regular Beta, which has an external surface area of $96 \text{ m}^2 \text{ g}^{-1}$. This is reflected in the catalytic results (Fig. 4) showing that the nanocrystalline sample is more active than the Beta-50 zeolite. We also carried out the reaction with a commercial Beta sample (Beta-CP811) that had a Si/Al ratio very close to that of Beta-n (see Table 1) and an average crystallite size of 150 nm, which is smaller than that for Beta-50 (500 nm). The results shown in Fig. 4 demonstrate that the nanocrystalline Beta zeolite deactivated slower and achieved a higher final conversion than the very acidic
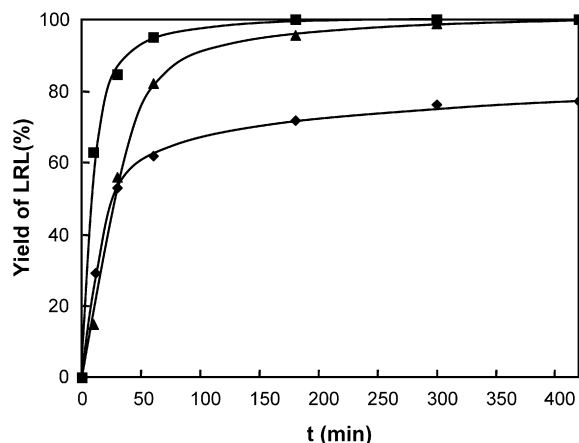
Fig. 7. Beckmann rearrangement of CDOX at 403 K over ITQ-2(25) in benzonitrile (■), chlorobenzene (▲) and 1,3,5-triisopropylbenzene (◆), with a catalyst/oxime ratio of 1:1 (wt/wt).

Beta-CP811. This behaviour was also found for other reactions in which the catalyst deactivates by accumulation of products into the pores [34].

3.1.2. Catalyst deactivation and influence of the solvent

In terms of the influence of time on stream on conversion, the results presented in Fig. 4 indicate that in most cases conversion does not reach 100%, but stops after a certain reaction time. This finding can be explained by assuming that some catalyst deactivation occurs, probably generated by strong adsorption of the lactam and some dimers that remain on the catalyst, blocking pores or active sites. Even if a batch system is not the best-suited reactor for studying catalyst deactivation, looking at the shape of the curves in Fig. 2, one would be inclined to say that the order of catalyst deactivation is ITQ-2 < MCM-41 < Beta-50. This order corresponds very well with the amount of organic remaining adsorbed on the catalyst after the reaction, which includes the organic extracted by Soxhlet plus the amount of organic remaining on the solid after extraction, and is 4 wt% for ITQ-2, 6 wt% for MCM-41, and 11 wt% for Beta-50. Also note that in the case of the nanocrystalline Beta (Beta-n), the total amount of organic on the catalyst was 8%, which is clearly less than the 11% obtained for the regular Beta zeolite.

At this point in our study, it was reasonable to assume that catalyst life, and consequently catalyst activity, could be improved if the adsorbed products could be removed during the reaction using a more polar solvent than chlorobenzene. To check this hypothesis, we performed the Beckmann rearrangement of CDOX at 403 K with ITQ-2(25) at a catalyst-to-oxime ratio of 1:1 (wt/wt) and using two solvents of very different polarity, 1,3,5-triisopropylbenzene and benzonitrile. The results, displayed in Fig. 7, show improved catalytic activity under the new reaction conditions. Indeed, using benzonitrile, 97% yield of lactam was obtained within 1 h of reaction time, whereas lower conversions were achieved when using chlorobenzene or the less polar solvent 1,3,5-triisopropylbenzene. Note that the amount of organic retained on the catalyst was 2 wt% when working with benzonitrile, compared with the 4 wt% observed with chlorobenzene. Consequently, it seems clear to us that the
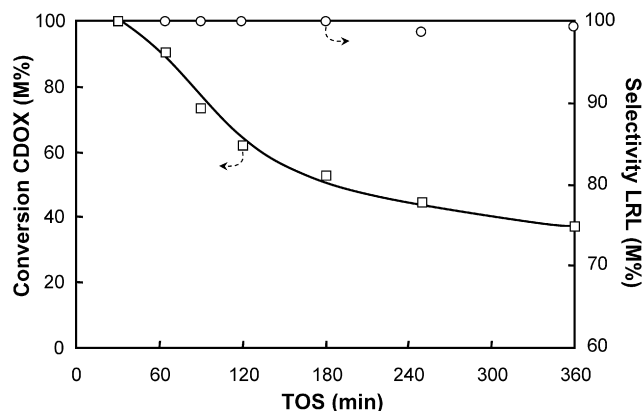

Fig. 8. Conversion of CDOX (□) and selectivity to LRL (○) in the continuous liquid-phase Beckmann rearrangement over ITQ-2(25). Experimental conditions as in Table 3.

liquid-phase Beckmann rearrangement of CDOX could be performed with solid acid catalysts, provided that the acidity and accessibility are tuned to allow rapid diffusion and desorption of products, which is also influenced by using a solvent with the appropriate polarity.

3.2. Beckmann rearrangement of CDOX in a continuous fixed-bed reactor: Catalytic deactivation and regeneration

From a process standpoint, one can certainly envision a slurry-type reactor in which fresh catalyst is continuously introduced and removed to compensate for catalyst deactivation. Nevertheless, and depending on the loss of catalytic activity, one can also consider parallel fixed-bed reactors in which reaction and regeneration alternate, or a catalyst moving bed if the deactivation is too fast. To better study catalyst deactivation, we performed the Beckmann rearrangement of CDOX in a fixed-bed reactor.

Fixed-bed experiments with ITQ-2(25) at 393 K using 1,2,4-trimethylbenzene as a solvent show an initial CDOX conversion and selectivity to LRL of 100% (Fig. 8). Rapid catalyst deactivation is observed, however, with conversion on dropping to <50% after 4 h TOS. According to studies carried out for the Beckmann rearrangement with other oximes [35–39], significant lactam adsorption can occur, leading to polymerization and eventually to coke. We studied the chloroform-extracted catalyst by ^{13}C CP-MAS-NMR spectroscopy and found that the organic deposit is formed mainly of LRL and/or its higher isomers. Fig. 9 shows the spectrum of the lactam characterized by four typical peaks: ^{13}C (75.0 MHz, CDCl$_3$) δ 25.7 ($C_{3–11}$), 42.0 (CH_2CO), 58.8 (CH_2NH), and 177.0 (CO). Other signals present correspond to some residue of 1,2,4-trimethylbenzene.

The important effect of lactam adsorption on the catalytic performance of ITQ-2 was corroborated by feeding a solution of LRL in 1,2,4-trimethylbenzene on an ITQ-2 catalyst within a fixed-bed reactor at 393 K up to saturation of the system. The findings, shown in Fig. 10, demonstrate that no product generated from LRL was detected at the outlet. But after the catalyst was washed with fresh solvent, CDOX was reacted; and the results (Table 3, Fig. 11) show that by passing LRL previously

Table 3
Beckmann rearrangement of CDOX in liquid-phase over ITQ-2(25) in a fixed-bed reactor. Influence of the adsorption of LRL in catalytic performance[a]

Catalyst	TOS = 30 min			Complete process (4 h)		
	$X_{T\ CDOX}$ (M%)[b]	S_{LRL} (M%)[b]	S_{CD} (M%)[b]	$X_{T\ CDOX}$ (M%)[c]	S_{LRL} (M%)[c]	S_{CD} (M%)[c]
Fresh	100	100	0	65	99.6	0.4
LRL-adsorption	88	100	0	48	100	0

[a] Experimental conditions: solvent 1,2,4-trimethylbenzene; $T = 393$ K; $W/F = 8.0$ h; CAT = 1.00 g; flow rate = 2.50 g h^{-1}; feed: CDOX 5 wt%.
[b] Initial conversion and selectivity.
[c] Data corresponding to the complete process (4 h).
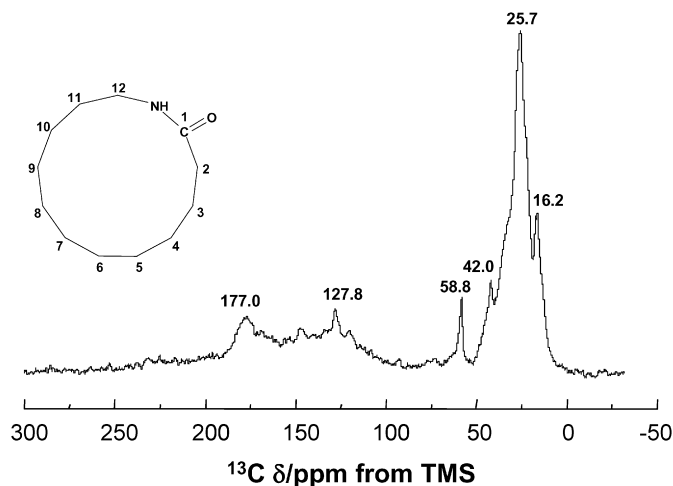
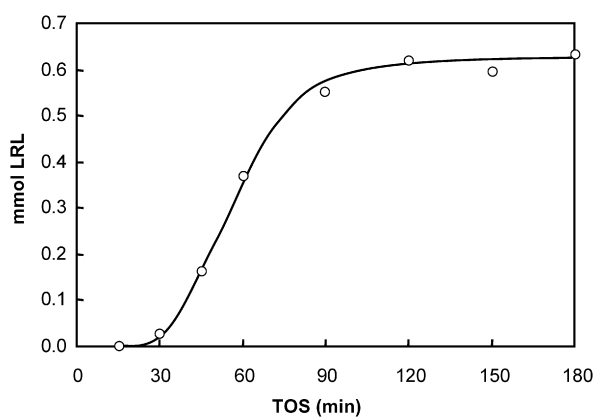Fig. 9. ^{13}C CP-MAS-NMR spectrum of the reaction used ITQ-2(25) catalyst.

Fig. 10. Adsorption of LRL on ITQ-2(25) in a fixed-bed reactor. Experimental conditions: solvent 1,2,4-trimethylbenzene; $T = 393$ K; $W/F = 15.3$ h; CAT: 1.00 g; flow rate: 5.03 g h^{-1}; feed: LRL 1.3 wt%.
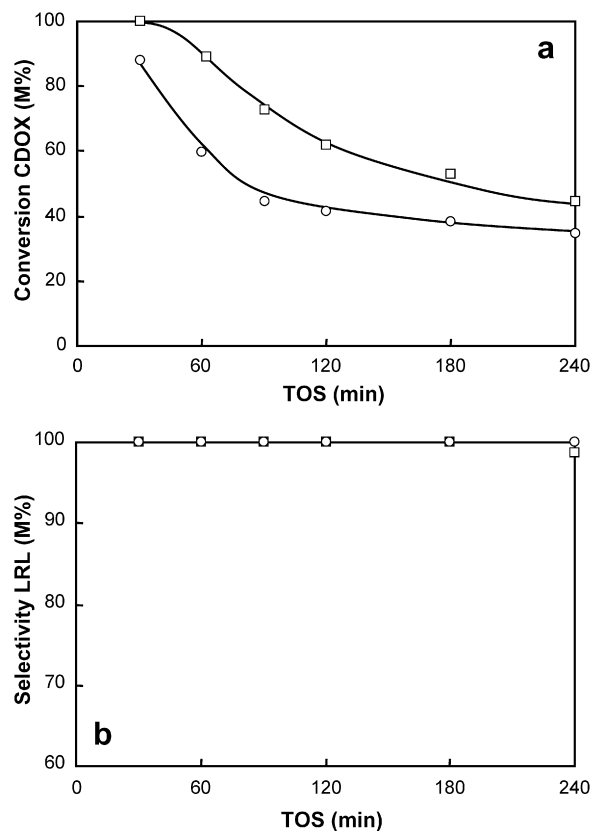

Fig. 11. Beckmann rearrangement of CDOX in liquid phase over fresh ITQ-2(25) (□) and LRL-adsorbed ITQ-2(25) (○). Influence of LRL adsorption in CDOX conversion (a) and selectivity to LRL (b) in a fixed-bed reactor. Experimental conditions as in Table 3.

to the reaction, the catalyst has lost more than 25% of activity. According to Tatsumi and co-workers [39], the lactam can be strongly adsorbed on strong Brønsted acid sites, resulting in rapid deactivation. Moreover, the formation of high-molecular-weight byproducts on strong acid sites by oligomerization of the lactam involves generation of water, which also contributes to catalytic decay and a loss of selectivity by hydrolysis of the reagent.

Because catalytic deactivation occurs rapidly in the liquid-phase rearrangement, we paid special attention to optimizing the experimental conditions to extend the catalyst life. As we saw before when working in a batch reactor, the nature of the solvent is an important variable. Indeed, it is generally accepted that the solvent can intervene in the stabilization of the activated complex in the rate-controlling step, the 1,2-H shift, to give the protonated oxime [40]. Moreover, the solvent can be adsorbed on the surface of a solid acid catalyst and, consequently, it competes with the reagent and products for the active sites. In this sense, nonprotic solvents with moderate dielectric constant and low basicity keep the adsorption–desorption equilibrium at a
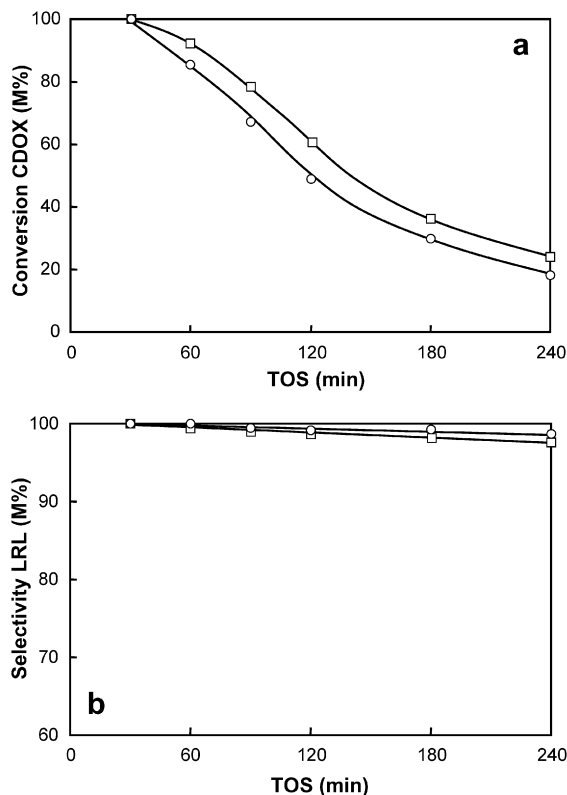
Fig. 12. Conversion of CDOX (a) and selectivity to LRL (b) in the continuous liquid-phase Beckmann rearrangement over ITQ-2(25) in benzonitrile (□) and 1,2,4-trimethylbenzene (○). Experimental conditions as in Table 4.
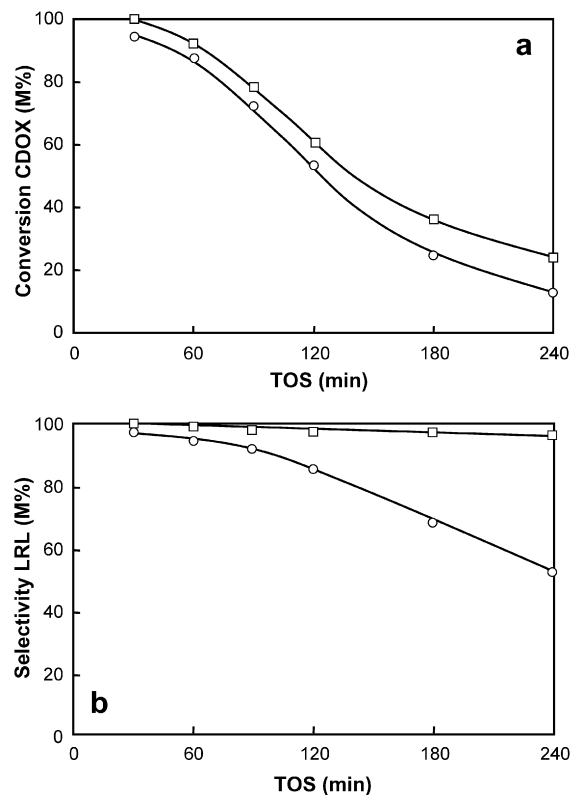
Fig. 13. Conversion of CDOX (a) and selectivity to LRL (b) in the continuous liquid-phase Beckmann rearrangement over ITQ-2(25) (■) and commercial Beta-CP811 (○). Experimental conditions as in Table 5.

Table 4
Beckmann rearrangement of CDOX in liquid-phase over ITQ-2(25) in a fixed-bed reactor. Influence of the solvent in catalytic performance[a]

Catalyst	TOS = 30 min			Complete process (4 h)		
	$X_{T\,CDOX}$ (M%)[b] NOH	S_{LRL} (M%)[b]	S_{CD} (M%)[b]	$X_{T\,CDOX}$ (M%)[c] NOH	S_{LRL} (M%)[c]	S_{CD} (M%)[c]
1,2,4-TMB	100	100	0	42	99.2	0.8
BN	100	100	0	54	97.8	2.2

[a] Experimental conditions: $T = 423$ K; $W/F = 4.0$ h; CAT = 1.00 g; flow rate = 8.33 g h^{-1}; feed: CDOX 3 wt%.
[b] Initial conversion and selectivity.
[c] Data corresponding to the complete process (4 h).

Table 5
Beckmann rearrangement of CDOX in liquid phase over ITQ-2(25) and commercial Beta-CP811 in a fixed-bed reactor[a]

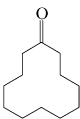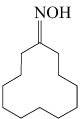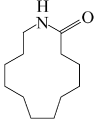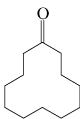| Catalyst	TOS = 30 min				Complete process (4 h)			
	$X_{T\,CDOX}$ (M%)[b] NOH	S_{LRL} (M%)[b]	S_{CD} (M%)[b]	S_{Others} (M%)[c]	$X_{T\,CDOX}$ (M%)[c] NOH	S_{LRL} (M%)[c]	S_{CD} (M%)[c]	S_{Others} (M%)[c]
ITQ-2(25)	100	100	0	0	54	97.8	2.2	0
Beta-CP811	94	97.0	3.0	0	35	80.6	9.8	9.7
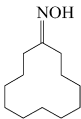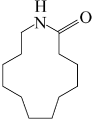
[a] Experimental conditions: solvent benzonitrile; $T = 423$ K; $W/F = 4.0$ h; CAT = 1.00 g; flow rate = 8.33 g h^{-1}; feed: CDOX 3 wt%.
[b] Initial conversion and selectivity.
[c] Data corresponding to the complete process (4 h).

Table 6
Beckmann rearrangement of CDOX in liquid phase over ITQ-2(25) in a fixed-bed reactor. Influence of catalyst regeneration[a]

Catalyst	TOS = 30 min			Complete process (4 h)		
	$X_{\text{T CDOX}}$ (M%)[b]	S_{LRL} (M%)[b]	S_{CD} (M%)[b]	$X_{\text{T CDOX}}$ (M%)[c]	S_{LRL} (M%)[c]	S_{CD} (M%)[c]
Fresh	100	100	0	65	99.6	0.4
Regenerated	97	100	0	71	100	0

[a] Experimental conditions: solvent 1,2,4-trimethylbenzene; $T = 393$ K; $W/F = 8.0$ h; CAT = 2.50 g; flow rate = 6.25 g h^{-1}; feed: CDOX 5 wt%.
[b] Initial conversion and selectivity.
[c] Data corresponding to the complete process (4 h).

level that can be beneficial for removing the synthesized LRL from the acid sites [41]. Then, as was seen before, benzonitrile seems to effectively promote desorption of the lactam, increasing the reaction rate and avoiding the formation of heavier basic products on strong acid sites. Accordingly, we compared the catalytic performance of ITQ-2(25) with benzonitrile and 1,2,4-trimethylbenzene as solvents. The results, given in Fig. 12 and Table 4, indicate significantly improved catalytic activity when using benzonitrile instead of 1,2,4-trimethylbenzene. Note, however, that traces of benzamide formed by hydrolysis of benzonitrile are detected. It then becomes important for the process to avoid any hydrolysis of the oxime or the benzonitrile.

Comparing the catalytic performance of ITQ-2(25) with a commercial sample of Beta (Beta-CP811) reveals a slightly faster deactivation in the zeolite (Fig. 13). Moreover, catalytic decay in this sample involves the loss of selectivity to LRL (Table 5). In fact, Tatsumi co-workers [42] described how the Beckmann rearrangement of cyclohexanone oxime over USY zeolite occurs on the weak Brønsted acid sites. However, as catalytic deactivation occurs, two secondary reactions gain importance: (1) the formation of high-molecular-weight byproducts on strong acid sites, with the subsequent production of water, and (2) the hydrolysis of the oxime with the water formed on weak Lewis acid sites. In our case, we found significant production of dimers of CDOX and CD on the Beta sample, always higher than that with ITQ-2(25), when decreasing catalytic activity (Table 5, S_{Others}).

Despite the fact that a more appropriate solvent gives higher catalytic activity and longer catalyst life, the catalyst still deactivates and regeneration is required. Then, to remove the organic compounds irreversibly adsorbed on ITQ-2, the sample was calcined in air at 813 K. This thermal treatment allows complete combustion of the organic deposit, and the regenerated catalyst practically recovers the initial activity and selectivity (see Table 6).

4. Conclusion

In contrast to what occurs with cyclohexanone oxime, it is not possible to perform the Beckmann rearrangement of cyclododecanone oxime in vapor phase due to molecular decomposition unless the process is carried out under vacuum [18]. In this sense, the liquid-phase rearrangement in batch and fixed-

bed continuous-flow reactors has demonstrated the importance of site accessibility for this reactant. In the case of large-pore zeolites (Beta), even when the crystal size was substantially reduced (20 nm), significant diffusion limitations for reactant and product exist, with a negative impact on activity and catalyst life. MCM-41, despite its large pores, is not active enough for this process. Conversely, a much better activity with 100% selectivity to laurolactam is found on the delaminated material ITQ-2 when site accessibility (i.e., level of delamination) and acid strength are optimized. Catalyst deactivation occurs due to irreversibly adsorbed ω-laurolactam and its higher homologues. In this sense, the nature of the solvent plays an important role for the desorption of the product and, consequently, increases catalyst lifetime. Consequently, when carrying out the process at higher temperatures in vacuum, ITQ-2 can be expected to have a longer life than Beta zeolite.

Acknowledgments

References

[1] W.F. Hölderich, J. Röseler, G. Heitmann, A.T. Liebens, Catal. Today 37 (1997) 353.
[2] P.S. Landis, P.B. Venuto, J. Catal. 6 (1996) 245.
[3] A. Aucejo, M.C. Burguet, A. Corma, V. Fornés, Appl. Catal. 22 (1986) 187.
[4] L.X. Dai, R. Hayasaka, Y. Iwaki, K.A. Koyano, T. Tatsumi, Chem. Commun. (1996) 1071.
[5] M.A. Camblor, A. Corma, H. García, V. Semmer-Herlédan, S. Valencia, J. Catal. 177 (1998) 267.
[6] R. Millini, G. Perego, W.O. Parker, G. Bellussi, L. Carluccio, Microporous Mater. 9 (1995) 221.
[7] M.E. Leonowicz, J.A. Lawton, S.L. Lawton, M.K. Rubin, Science 264 (1994) 1910.
[8] J. Röseler, G. Heitmann, W.F. Hölderich, Stud. Surf. Sci. Catal. 105 (1996) 1173.
[9] J. Röseler, G. Heitmann, W.F. Hölderich, Appl. Catal. A Gen. 144 (1996) 319.
[10] T. Takahashi, K. Ueno, T. Kai, J. Chem. Eng. 69 (1991) 1096.
[11] H. Sato, N. Ishii, K. Hirose, S. Nakamura, Stud. Surf. Sci. Catal. 28 (1996) 755.
[12] H. Sato, K. Hirose, S. Nakamura, Stud. Surf. Sci. Catal. 49 (1989) 1213.

[13] H. Sato, K. Hirose, S. Nakamura, Chem. Lett. (1993) 1987.
[14] T. Yashima, K. Miura, T. Komatsu, Stud. Surf. Sci. Catal. 84 (1994) 1897.
[15] W.F. Hölderich, Stud. Surf. Sci. Catal. 46 (1989) 193.
[16] L.X. Dai, K. Koyama, T. Tatsumi, Catal. Lett. 53 (1998) 211.
[17] R. Palkovits, C.M. Yang, S. Olejnik, F. Schueth, J. Catal. 243 (2006) 93.
[18] E. Lacroix, S. Hub, W. Holderich, W. Eickelberg, F. Fajula, F. Di Renzo, M. Brandhorst, WO Patent 2006136699 (2006).
[19] K. Ishihara, JP Patent 2006219470 (2006).
[20] Y. Fukuda, Y. Yamamoto, A. Haruta, JP Patent 2006151911 (2006).
[21] (a) S. Yamamoto, A. Haruta, Y. Fukuda, JP Patent 2005023014 (2005);
(b) Y. Yamamoto, A. Haruta, Y. Fukuda, WO Patent 2005063388 (2005).
[22] A. Corma, M.J. Díaz-Cabañas, J.L. Jordá, C. Martínez, M. Moliner, Nature 443 (2006) 842.
[23] A. Corma, V. Fornés, S.B. Pergher, Th.L.M. Maesen, J.G. Buglass, Nature 376 (1998) 353.
[24] (a) A. Corma, U. Diaz, M.E. Domine, V. Fornés, Angew. Chem. Int. Ed. 38 (2000) 1499;
(b) A. Corma, U. Diaz, M.E. Domine, V. Fornés, J. Am. Chem. Soc. 122 (2000) 2804.
[25] M.K. Rubin, P. Chu, US Patent 4954325 (1990).
[26] (a) L. Schreyeck, P.H. Caulet, J.C. Mongenel, J.L. Guth, B. Marler, Chem. Commun. 2187 (1995);
(b) L. Schreyeck, P.H. Caulet, J.C. Mongenel, J.L. Guth, B. Marler, Microporous Mater. 6 (1996) 259.
[27] C.T. Kresge, M.E. Leonowicz, W.J. Roth, J.C. Vartulli, J.S. Beck, Nature 359 (1992) 710.
[28] S. Valencia, Ph.D. thesis, CSIC-UPV (1997).
[29] M.A. Camblor, A. Corma, A. Mifsud, J. Pérez-Pariente, S. Valencia, Stud. Surf. Sci. Catal. 105 (1997) 341.
[30] L. Vogel, A Text Book of Practical Organic Chemistry, Longmann, London, 1971.
[31] J.S. Reddy, R. Ravishankar, P. Ratnasamy, Catal. Lett. 17 (1993) 139.
[32] W.K. Bell, C.D. Chang, Eur. Pat. Appl. EP056698 (1985).
[33] A.B. Fernández, M. Boronat, T. Blasco, A. Corma, Angew. Chem. Int. Ed. 44 (2005) 2370.
[34] P. Botella, A. Corma, J.M. López-Nieto, S. Valencia, R. Jacquot, J. Catal. 195 (2000) 161.
[35] T. Tatsumi, in: R.A. Sheldon, H. van Bekkum (Eds.), Fine Chemicals through Heterogeneous Catalysis, Wiley–VCH, Weinheim, 2001, p. 185.
[36] T. Curtin, J.B. McMonagle, B.K. Hodnett, Appl. Catal. A Gen. 93 (1992) 91.
[37] P. Albers, K. Saibold, T. Haas, G. Prescher, W.F. Hölderich, J. Catal. 176 (1998) 571.
[38] N. Kob, R.S. Drago, Catal. Lett. 49 (1998) 49.
[39] (a) C. Ngamcharussrivichai, P. Wu, T. Tatsumi, J. Catal. 227 (2004) 448;
(b) C. Ngamcharussrivichai, P. Wu, T. Tatsumi, J. Catal. 235 (2005) 139;
(c) C. Ngamcharussrivichai, P. Wu, T. Tatsumi, Appl. Catal. A Gen. 288 (2005) 158.
[40] M.T. Nguyem, G. Raspoet, L.G. Vanquickenborne, J. Am. Chem. Soc. 199 (1997) 2552.
[41] (a) Y.M. Chung, H.Y. Rhee, J. Mol. Catal. A Chem. 159 (2000) 389;
(b) Y.M. Chung, H.Y. Rhee, J. Mol. Catal. A Chem. 175 (2001) 249.
[42] C. Ngamcharussrivichai, P. Wu, T. Tatsumi, J. Catal. 235 (2005) 139.
[43] C.A. Emeis, J. Catal. 141 (1993) 347.